

Highlighting research results from Prof. Y. T. Matsunaga and co-workers from The University of Tokyo, Tokyo, Japan.

Multiwalled carbon nanotube reinforced biomimetic bundled gel fibres

Biomimetically designed bundled gel fibres containing hydroxypropyl cellulose (HPC) were reinforced with multi-walled carbon nanotubes (MWCNT). Their good parallel morphology and enhanced mechanical/electrical properties provide an appropriate cell cultivation environment.

As featured in:



See Yukiko T. Matsunaga et al., *Biomater. Sci.*, 2016, 4, 1197.



[www.rsc.org/biomaterialsscience](http://www.rsc.org/biomaterialsscience)

Registered charity number: 207890



Cite this: *Biomater. Sci.*, 2016, **4**, 1197

Received 27th April 2016,  
Accepted 12th May 2016

DOI: 10.1039/c6bm00292g

www.rsc.org/biomaterialsscience

## Multiwalled carbon nanotube reinforced biomimetic bundled gel fibres†

Young-Jin Kim,<sup>a,b</sup> Seiichiro Yamamoto,<sup>a,c</sup> Haruko Takahashi,<sup>a</sup> Naruo Sasaki<sup>c,d</sup> and Yukiko T. Matsunaga<sup>\*a</sup>

**This work describes the fabrication and characterization of hydroxypropyl cellulose (HPC)-based biomimetic bundled gel fibres. The bundled gel fibres were reinforced with multiwalled carbon nanotubes (MWCNTs). A phase-separated aqueous solution with MWCNT and HPC was transformed into a bundled fibrous structure after being injected into a co-flow microfluidic device and applying the sheath flow. The resulting MWCNT-bundled gel fibres consist of multiple parallel microfibrils. The mechanical and electrical properties of MWCNT-bundled gel fibres were improved and their potential for tissue engineering applications as a cell scaffold was demonstrated.**

Fibrous materials have a major role to play in the rapidly expanding field of biotechnology.<sup>1–4</sup> In particular, distinctive fibrous structures, such as hollow fibres, fibre webs and bundled gel fibres, have attracted much attention because of their biomimetic structures and a wide range of biotechnological applications.<sup>5–7</sup> Many efforts to fabricate biomimetic structured cell culture scaffolds and evaluate their biocompatibility have been reported over the last few decades because biomimetic scaffolds have potential to be widely applicable to the fields of tissue engineering and regenerative medicine.<sup>8–10</sup> Here, we focus on the bundled gel fibres, which could potentially be used for soft tissue engineering owing to their interesting fibrous biomimetic morphology; the fibres consist of many small microfibrils and are highly uniform, continuous, parallel, and long. This structure is very similar to that of

tissues such as muscles, tendons and nerves. One of the most interesting approaches to fabricate fibrous gel fibres is using a microfluidic device, which is a simple process that is cost-effective compared with other methods such as electrospinning, drawing, and self-assembly.<sup>11–13</sup> Recently, we reported a method for generating hydroxypropyl cellulose (HPC) bundled gel fibres using a co-flow microfluidic device.<sup>14</sup> The bundled fibrous structure can be generated by applying the sheath flow to the phase-separated polymer solution in the microchannel. The phase separation of the polymer-rich and solvent-rich regions in the polymer blend solution is a requisite for the generation of the bundled fibrous structures because the polymer-rich phase is elongated and then finally transformed into the bundled fibrous structure *via* the sheath flow.<sup>15</sup> Furthermore, we demonstrated the potential applicability of these bundled gel fibres as a scaffold for soft tissue engineering in a cell culture study.

However, those bundled gel fibres lacked certain desirable mechanical and electrical properties, which need to be introduced in next generation bundled gel fibres for these materials to reach their full potential. This research therefore employs multiwalled carbon nanotubes (MWCNTs) to enhance the material's mechanical and electrical properties, which are important for biotechnological applications.<sup>16–18</sup> MWCNTs have extremely high aspect ratio, mechanical strengths and electrical conductivities; they strongly influence the properties of polymeric matrices they are embedded in.<sup>19–21</sup> Here, we describe the generation of MWCNT-incorporated HPC bundled gel fibres using a phase-separated HPC-based solution and co-flow microfluidic device (Fig. S1A†); further, we studied the effect of MWCNTs on the material's mechanical and electrical properties and compared the cell culture results of bundled gel fibres with and without MWCNTs (Fig. 1). HPC, one of the most representative naturally derived polysaccharide cellulosic polymers, is widely used in biomedical applications such as in cell culture scaffolds and drug delivery systems because of its high biocompatibility.<sup>22–24</sup> However, HPC bundled gel fibres are unstable in aqueous solutions without employing a cross-linking process. The cross-linking process,

<sup>a</sup>Center for International Research on Integrative Biomedical Systems (CIBiS), The University of Tokyo, 4-6-1 Komaba, Meguro-ku, Tokyo, 153-8505, Japan. E-mail: mat@iis.u-tokyo.ac.jp

<sup>b</sup>Japan Society for the Promotion of Science (JSPS), 8 Ichibancho, Chiyoda-ku, Tokyo, 102-8472, Japan

<sup>c</sup>Department of Materials and Life Science, Seikei University, 3-3-1 Kichijoji Kitamachi, Musashino, Tokyo, 180-8633, Japan

<sup>d</sup>Department of Applied Physics, Faculty of Informatics and Technology, The University of Electro-Communications, 1-5-1 Chofugaoka, Chofu, Tokyo 182-8585, Japan

†Electronic supplementary information (ESI) available. See DOI: 10.1039/c6bm00292g



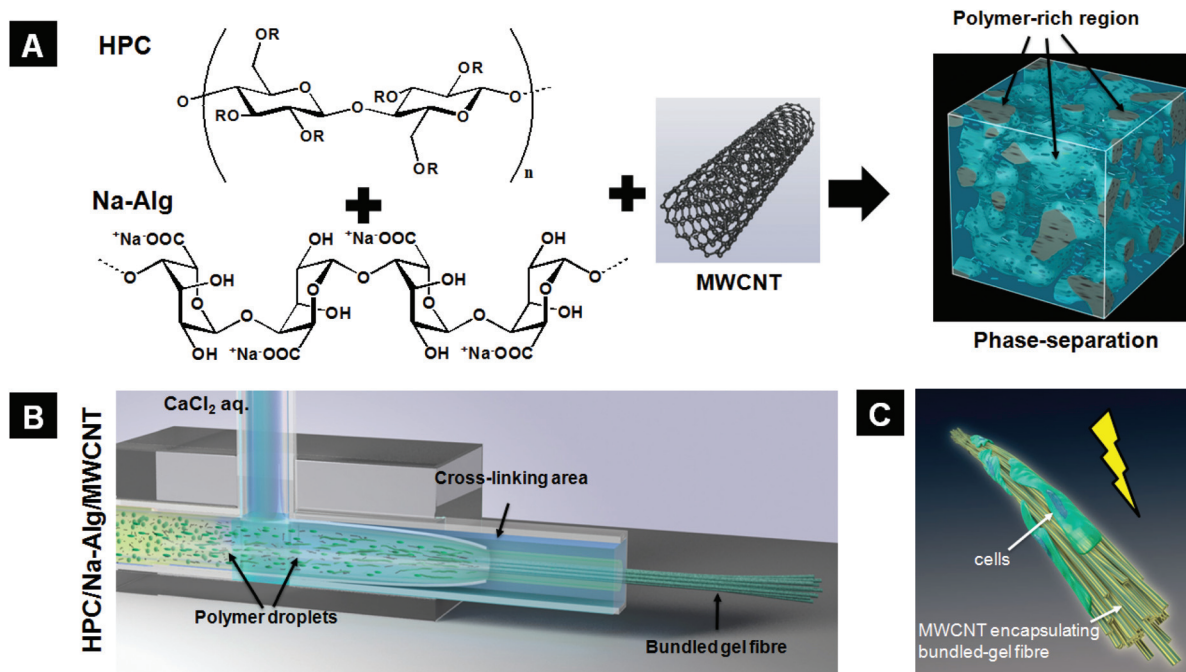


**Fig. 1** (A) Illustration of preparation of phase-separated HPC/Na-Alg/MWCNTs in aqueous solution. Polymer blend solutions are phase-separated and divided into polymer-rich and polymer-poor regions by adjusting temperature and pH. Na-Alg is employed as both a phase-separating agent that induces a salting-effect in the polymer solution and a cross-linking assistant to temporarily cross-link the resultant bundled fibrous structure. (B) Illustration for generation of bundled gel fibres using the co-flow microfluidic device, phase-separated polymer blend, and cross-linker. The polymer-rich regions are elongated by the sheath flow in the microchannel and then form the bundled fibrous structure. This structure is stably obtained *via* a cross-linking process in the microchannel. (C) The bundled gel fibres could potentially be used in the field of soft tissue engineering for cell culture scaffolds with electrical stimuli.

therefore, is required to maintain the bundled structure, but the HPC cross-linking process takes over a day to complete. Here, we employed a polysaccharide polymer, sodium alginate (Na-Alg), as a cross-linker because it acts rapidly in the presence of calcium chloride ( $\text{CaCl}_2$ ) solution (Fig. S1B and C†). Temporarily cross-linked bundled gel fibres are stable and offer enough time for the HPC molecules to be cross-linked by immersing in divinyl sulfone (DVS) solution.

The aqueous phase-separated solution was prepared by mixing HPC (7 wt%), Na-Alg (1 wt%), and MWCNTs (0.00, 0.01, and 0.05%). The most important parameter to consider for bundled gel fibres is the solution's pH value, which greatly influences the phase separation *via* the "salting-out" effect.<sup>25,26</sup> Here, we adjusted the pH of the polymer solution to 13 to induce phase separation. As shown in Fig. S2,† the polymer blend solution displays a homogeneous structure, and no phase separation was observed in the MWCNTs/HPC/Na-Alg reference solution with pH 7 at 28 °C. In addition, MWCNT aggregation and precipitation were observed; to avoid these phenomena, the MWCNTs were oxidized using sulfuric acid, nitric acid, and hydrochloric acid. After oxidation, the MWCNTs' zeta-potential decreased from  $-23.4 \pm 2.6$  to  $-33.4 \pm 4.0$  mV. The pH also decreased from 6.8 to 3.7. Oxidized MWCNTs were dispersed well in the polymer blend solution *via* repulsion forces between the nanotubes and no phase separation was observed for pH 7 solutions at 28 °C (Fig. 2A).

With a pH of 13, conversely, phase separation was clearly visible. The polymer-rich and polymer-poor phases occurred without MWCNTs (data not shown) and with MWCNTs at 28 °C (Fig. 2B). The polymer-rich phase appeared as polymer droplets around 25 °C and gradually increased in volume with increasing temperature, up to 28 °C, when the polymer droplets formed networks. We attribute this to a combination of a "salting-out" effect and HPC's temperature-responsiveness. First, added sodium ions, which act as a salt, take water molecules; consequently, the solubility of HPC and Alg in water is decreased. Therefore, the polymer was extracted and concentrated by increasing the interactions between the two polymers. Second, a unique feature of HPC is its temperature-responsivity in aqueous solutions, which allows a reversible coil-globule transition in response to temperature alternations over its lower critical solution temperature (LCST, near 42 °C).<sup>27,28</sup> Below its LCST, HPC forms strong hydrogen bonds with water molecules; conversely, above its LCST HPC molecules expel water molecules. However, its LCST can be moved to around 25 °C by adjusting the solution's pH value to 13. In our experiments the polymer-rich areas were therefore gradually expanded *via* expulsion of water molecules by HPC when the solution temperature was increased above its LCST. In general, carboxylic acid can dissociate in an aqueous solution and then generate new hydrogen bonds. The oxidized MWCNTs, therefore, disturb phase separation when the



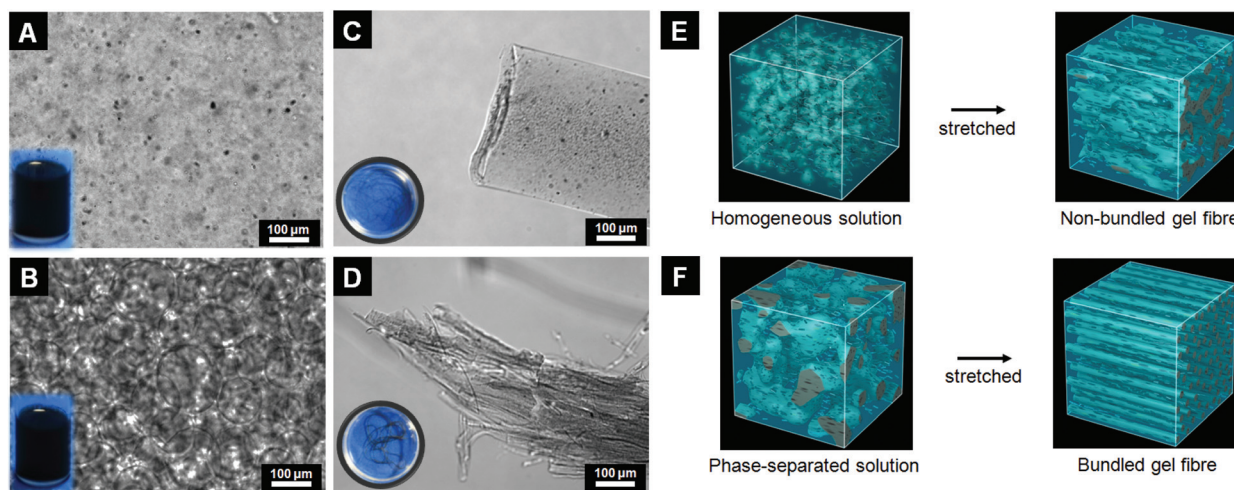


**Fig. 2** Microscopic images of HPC/Na-Alg polymer blend in aqueous solution with oxidized-MWCNTs at 28 °C ((A) pH 7 and (B) pH 13). Cross sectional microscope images of resultant fibres under the sheath flow using a co-flow microfluidic device ((C) non-bundled gel fibre from pH 7 solution and (D) bundled gel fibre from pH 13 solution). (E) and (F) illustrate the generation mechanisms for non-bundled gel fibres and bundled gel fibres from a homogeneous solution (pH 7) and phase-separated solution (pH 13) in the microchannel, respectively.

concentration of polymers is low (5 wt% of HPC and 1 wt% of Alg). In this regard, we employed 7 wt% of HPC and 1 wt% of Alg solution for generation of MWCNT-incorporated bundled gel fibres because increased concentration of polymers could eliminate the disturbance effect of hydrogen bonds by dissociated carboxylic acid from oxidized MWCNTs.

We fabricated MWCNT-incorporated bundled gel fibres using a co-flow microfluidic device and a MWCNT-containing phase-separated solution by applying the sheath flow. Briefly, the polymer blend (pH 7 and 13) and an aqueous solution of  $\text{CaCl}_2$  (as a cross-linker) were injected into the inner and outer channels, respectively. The flow rates were set at  $300 \mu\text{l min}^{-1}$  and  $2500 \mu\text{l min}^{-1}$  for the polymer blend solution and cross-linker, respectively. The fibre was obtained from the outlet after applying the sheath flow in the two channels simultaneously. The resultant fibres were immediately placed into the DVS solution to cross-link the HPC molecules. Finally, unreacted Na-Alg molecules were removed by soaking in a trisodium citrate solution. The morphologies of the obtained fibres were analyzed using a phase-contrast microscope and scanning electron microscope (SEM). Fibres obtained from MWCNTs/HPC/Na-Alg solution at pH 7 were non-bundled single-string MWCNT-incorporated microfibres (Fig. 2C and S3A†); the MWCNTs were uniformly dispersed in these gel fibres, which were approximately 200–250  $\mu\text{m}$  in diameter. This finding was also confirmed *via* a SEM image (Fig. S3B†). We attribute this to the lack of sources for bundled structures in the homogeneous polymer solution (Fig. 2E). Conversely, fibres have a bundled structure when using a phase-separated HPC/Alg solution at pH 13. This structure was also observed in a cross sectional image, which shows that the large fibres consist of many multi-parallel small microfibres of 1–3  $\mu\text{m}$  in diameter (Fig. 2D and S3C†). The bundled structure was also visible in a SEM image (Fig. S3D†). We propose that the phase-

separated polymer droplets are each separately elongated to form the bundled structure under the sheath flow (Fig. 2F).

MWCNTs enhance multiple material properties owing to their extremely high tensile strength, stiffness and high electrical conductivity. In particular, reinforced polymer matrices with MWCNTs show remarkably improved mechanical properties. Here, we also demonstrated enhanced material properties by using MWCNTs in HPC fibres by measuring their tensile strength, elastic modulus and conductivity. The mechanical strength of the fibres was measured by using a tensile tester. All samples exhibited a linear elastic behaviour. The tensile strength results of MWCNT-incorporated bundled gel fibres, MWCNT-incorporated non-bundled gel fibres, and bundled gel fibres were  $46.6 \pm 6.95$ ,  $18.8 \pm 1.59$ , and  $20.1 \pm 4.99$  kPa, respectively, as shown in Fig. 3A. The tensile strength of the bundled gel fibres was approximately doubled by adding 0.5% of MWCNTs compared with no MWCNTs. The MWCNTs' reinforcing effect was also confirmed: the elastic modulus of the MWCNT-incorporated bundled gel fibres was  $26.3 \pm 7.30$ , whereas without MWCNTs it was only  $18.9 \pm 6.10$ , Fig. 3B. Our previous study demonstrated that bundled gel fibres show higher mechanical strength compared to non-bundled gel fibres even without MWCNTs.<sup>14</sup> We assume that the multiple parallel fibres of the bundled structure reduced the applied tensile loads by deconcentrating the loads into the many small microfibres. Our finding in this study shows that we could successfully control the mechanical properties of the bundled gel by simply incorporating MWCNTs.

For soft tissue engineering with muscle and nerve tissues, the electrical conductivity of scaffolds would be one of the interesting features because electrical signals can strongly influence the cell signal pathway, growth, spreading and communications.<sup>29,30</sup> The current density–voltage ( $I$ – $V$ ) curves for three samples were obtained using a picoammeter and are



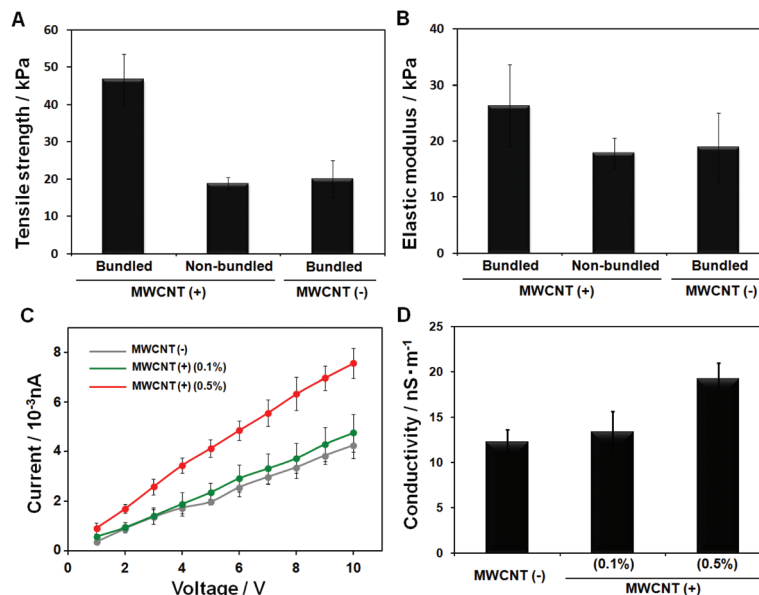


**Fig. 3** Mechanical and electrical characterization of gel fibres. (A) Tensile strength and (B) elastic modulus of MWCNT-incorporated bundled gel fibres, MWCNT-incorporated non-bundled gel fibres and bundled gel fibres were measured using a universal testing machine at 25 °C in a humid environment. (C) The  $I$ - $V$  curves for bundled gel fibres (with 0.0, 0.1 and 0.5% of MWCNTs) were measured using a picoammeter with a two-point probe at 25 °C, respectively. (D) Electrical conductivity was calculated from the results of picoammeter measurement.

shown in Fig. 3C: fibres containing 0.0, 0.1, and 0.5% MWCNTs. We found electrical conductivity improvements with increasing MWCNT concentrations in the bundled gel fibres:  $12.23 \pm 1.35$  (0.0%) and  $13.37 \pm 2.25$  (0.1%) to  $19.20 \pm 1.72$  (0.5%)  $\text{nS m}^{-1}$ , as shown in Fig. 3D. Improved electrical conductivity was confirmed in MWCNT-incorporated bundled gel fibres compared with MWCNT-incorporated non-bundled gel fibres.

The potential of bundled gel fibres with 0.1 and 0.5% MWCNTs for use as cell culture scaffolds was evaluated in a cell culture study. We used normal human dermal fibroblasts (NHDFs), and all images were taken after immunostaining for F-actin and nuclei by confocal laser scanning microscopy (CLSM). We confirmed cell attachment and spreading after

3 days of cultivation. By increasing the concentration of MWCNTs from 0.1 to 0.5%, initial cell attachment and cell spreading were improved (Fig. 4A and B). After 6 days of cultivation, NHDFs formed a cylinder-like shape, mimicking cylindrical tissue (Fig. 4C).

In conclusion, we have presented a simple method for generating biomimetic MWCNT-incorporated bundled gel fibres. Our method used a simple co-flow microfluidic device, where a phase-separated HPC/Alg polymer aqueous solution is subjected to shear stress to generate long continuous fibres that were a few hundred micrometers in diameter and had a bundled structure. Phase separation occurred when the pH value was increased to 13 because salt ( $\text{Na}^+$ ) ions induced a “salting-out” effect. Furthermore, we confirmed that

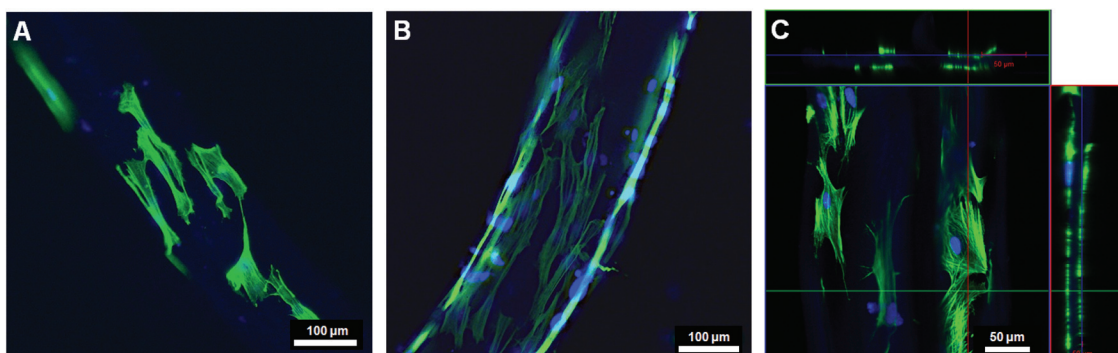


**Fig. 4** Immunofluorescent confocal images of NHDFs on the MWCNT-containing bundled gel fibres ((A) 0.1% and (B) 0.5% of MWCNTs) after 3 days of cultivation. (C) Cross-sectional image of MWCNTs-containing bundled gel fibres (0.5% of MWCNTs) after 6 days of cultivation. F-actin and nuclei were stained with Alexa488-conjugated phalloidin (green) and Hoechst33342 (blue), respectively.



the MWCNTs were homogeneously dispersed in the phase-separated polymer solution after oxidation. The bundled structure was formed from elongation of the polymer-rich regions of the phase-separated polymer solution; no bundled structure was observed with pH 7 polymer solution. Bundled gel fibres approximately 200–250  $\mu\text{m}$  in diameter were observed by using a phase-contrast microscope and SEM. Additionally, we confirmed that one bundled fibre consisted of many smaller parallel microfibrils each 1–3  $\mu\text{m}$  in diameter. The effects of MWCNTs on the mechanical and electrical properties were successfully demonstrated: tensile strength, elastic modulus, and electrical conductivity were improved with increasing concentrations of MWCNTs. In cell studies, MWCNT-incorporated bundled gel fibres supported initial cell attachment, spreading and growth, and cells formed a cylinder-like shape mimicking cylindrical tissue. These MWCNT-incorporated bundled gel fibres show great potential as cell culture scaffolds for use in soft tissue engineering and regenerative medicine.

## Acknowledgements

We thank Y. Takahashi for his technical assistance in preparing the bundled gel fibres and the tensile tests. We also thank M. Kumemura for her technical assistance in the electrical measurements of the gel fibres. We thank T. Ando for his contribution to the artwork. This work was partly supported by PRESTO, Japan Science and Technology (JST), Japan, Japan Society for the Promotion of Science (JSPS) KAKENHI: Grant-in-Aid for Young Scientists (A), Grant No. 25706010 to Y. T. M., Grant-in-Aid for JSPS Fellows, Grant No. 2503353 to Y. T. M. and the JSPS Core-to-Core Program. This research was also supported by Strategic International Research Cooperative Program, JST.

## Notes and references

- 1 C. Zhou, Q. Shi, W. Guo, L. Terrell, A. T. Qureshi, D. J. Hayes and Q. Wu, *ACS Appl. Mater. Interfaces*, 2013, **5**, 3847–3854.
- 2 Y.-J. Kim, M. Ebara and T. Aoyagi, *Adv. Funct. Mater.*, 2013, **23**, 5753–5761.
- 3 H. W. B. Joseph, *Philosophy*, 1938, **13**, 93–98.
- 4 Y.-J. Kim, M. Ebara and T. Aoyagi, *Angew. Chem., Int. Ed.*, 2012, **51**, 10537–10541.
- 5 W. E. Teo and S. Ramakrishna, *Nanotechnology*, 2005, **16**, 1878–1884.
- 6 S. Agarwal, A. Greiner and J. H. Wendorff, *Adv. Funct. Mater.*, 2009, **19**, 2863–2879.
- 7 Y.-J. Kim, M. Ebara and T. Aoyagi, *Sci. Technol. Adv. Mater.*, 2012, **13**, 064203.
- 8 S. Minardi, M. Sandri, J. O. Martinez, I. K. Yazdi, X. Liu, M. Ferrari, B. K. Weiner, A. Tampieri and E. Tasciotti, *Small*, 2014, **10**, 3943–3953.
- 9 J. M. Holzwarth and P. X. Ma, *Biomaterials*, 2011, **32**, 9622–9629.
- 10 Y.-J. Kim, M. Tachibana, M. Umezumi and Y. T. Matsunaga, *J. Mater. Chem. B*, 2016, **4**, 1740–1746.
- 11 D. Kiriya, R. Kawano, H. Onoe and S. Takeuchi, *Angew. Chem., Int. Ed.*, 2012, **51**, 7942–7947.
- 12 C. M. Hwang, A. Khademhosseini, Y. Park, K. Sun and S.-H. Lee, *Langmuir*, 2008, **24**, 6845–6851.
- 13 H. Onoe, T. Okitsu, A. Itou, M. Kato-Negishi, R. Gojo, D. Kiriya, K. Sato, S. Miura, S. Iwanaga, K. Kuribayashi-Shigetomi, Y. T. Matsunaga, Y. Shimoyama and S. Takeuchi, *Nat. Mater.*, 2013, **12**, 584–590.
- 14 Y.-J. Kim, Y. Takahashi, N. Kato and Y. T. Matsunaga, *J. Mater. Chem. B*, 2015, **3**, 8154–8161.
- 15 T. Hashimoto, K. Matsuzaka, E. Moses and A. Onuki, *Phys. Rev. Lett.*, 1995, **74**, 126–129.
- 16 X. Zhang, L. Meng and Q. Lu, *ACS Nano*, 2009, **3**, 3200–3206.
- 17 H. Zhang, Z. G. Wang, Z. N. Zhang, J. Wu, J. Zhang and J. S. He, *Adv. Mater.*, 2007, **19**, 698–704.
- 18 M. Okamoto and B. John, *Prog. Polym. Sci.*, 2013, **38**, 1487–1503.
- 19 R. H. Baughman, A. A. Zakhidov and W. A. de Heer, *Science*, 2002, **297**, 787–792.
- 20 J. Zhang, K. Qiu, B. Sun, J. Fang, K. Zhang, H. Eihamshary, S. S. Al-Deyab and X. Mo, *J. Mater. Chem. B*, 2014, **2**, 7945–7954.
- 21 S. Subramoney, *Adv. Mater.*, 1998, **10**, 1157–1171.
- 22 F. J. Xu, Y. Zhu, F. S. Liu, J. Nie, J. Ma and W. T. Yang, *Bioconjugate Chem.*, 2010, **21**, 456–464.
- 23 S. P. Hoo, Q. L. Loh, Z. Yue, J. Fu, T. T. Y. Tan, C. Choong and P. P. Y. Chan, *J. Mater. Chem. B*, 2013, **1**, 3107–3117.
- 24 Z. Aytac, H. S. Sen, E. Durgun and T. Uyar, *Colloids Surf., B*, 2015, **128**, 331–338.
- 25 H. Du, S. R. Wickramasinghe and X. Qian, *J. Phys. Chem. B*, 2013, **117**, 5090–5101.
- 26 M. J. Hey, D. P. Jackson and H. Yan, *Polymer*, 2005, **46**, 2567–2572.
- 27 M. Bagheri, S. Shateri, H. Niknejad and A. A. Entezami, *J. Polym. Res.*, 2014, **21**, 1–15.
- 28 A.-F. Metaxa, E. K. Efthimiadou, N. Boukos, E. A. Fragozeorgi, G. Loudos and G. Kordas, *J. Colloid Interface Sci.*, 2014, **435**, 171–181.
- 29 G. Cellot, F. M. Toma, Z. Kasap Varley, J. Laishram, A. Villari, M. Quintana, S. Cipollone, M. Prato and L. Ballerini, *J. Neurosci.*, 2011, **31**, 12945–12953.
- 30 A. Mazzatenta, M. Giugliano, S. Campidelli, L. Gambazzi, L. Businaro, H. Markram, M. Prato and L. Ballerini, *J. Neurosci.*, 2007, **27**, 6931–6936.

